Available online at www.sciencedirect.com

ScienceDirect

Ceramics International 40 (2014) 3799–3804

CERAMICS INTERNATIONAL

www.elsevier.com/locate/ceramint

The influence of the TiO_2 particle size on the properties of $Li_4Ti_5O_{12}$ anode material for lithium-ion battery

Dan Wang[a], Xiaoyan Wu[a], Yaoyao Zhang[b], Jin Wang[a], Peng Yan[a], Chunming Zhang[a,*], Dannong He[a,b,*]

[a]National Engineering Research Center for Nanotechnology, Shanghai 200241, China
[b]School of Material Science and Engineering, Shanghai Jiao Tong University, Shanghai 200240, China

Received 30 August 2013; received in revised form 10 September 2013; accepted 10 September 2013
Available online 16 September 2013

Abstract

The spinel $Li_4Ti_5O_{12}$ anode materials were prepared using high-energy ball milling assisted solid-state reaction method. In order to obtain the electrode materials with the best electrochemical performance, the influence of different TiO_2 particle sizes for $Li_4Ti_5O_{12}$ synthesis was systematically studied. The physical and electrochemical properties of the obtained samples were characterized by X-ray diffraction, scanning electron microscopy, Brunauer–Emmett–Teller surface area analysis, A.C. impedance, galvanostatic charge–discharge and cyclic voltammetry tests. The results showed that the initial particle size of TiO_2 played an important role on the properties of $Li_4Ti_5O_{12}$. It could affect the final grain size, the specific surface area, the electrochemical properties and the Li-ion diffusion coefficient of $Li_4Ti_5O_{12}$. Electrochemical testing results showed that the $Li_4Ti_5O_{12}$ prepared by TiO_2 with particle size of 25 nm exhibited the best electrochemical properties. The discharge capacity reached 164.7 mAh/g at 0.5 C. When the current rate was increased to 10 C, the first discharge capacity was only dropped to 70.6 mAh/g, and the capacity retention was 94.5% at the 50th cycle.

Keywords: Lithium-ion battery; Anode material; $Li_4Ti_5O_{12}$; TiO_2 particle size

1. Introduction

Lithium-ion batteries have been considered as an attractive power source for portable electronics, hybrid and plug-in hybrid electric vehicles due to their high power and energy densities. Recently, an ever-increasing research effort has been made to promote their application in hybrid electric vehicles and dispersed energy storage systems, which demand light weight, high power, high energy densities, high safety and long cycle-life [1,2]. Spinel $Li_4Ti_5O_{12}$, as a promising anode material for lithium-ion batteries, has attracted special attention due to its extremely small structural change during Li insertion/extraction and the absence of solid electrolyte interface film: its flat discharge platform at about 1.55 V versus Li^+/Li is above the reduction potential of most organic electrolytes which can restrain the passive films from the reduction of electrolytes and sufficiently avoid the formation of metallic lithium [3–5].

Besides the requirement of high structure stability, the electrochemical performance of the electrode is also closely related to its specific morphology. The morphology is closely dependent on the synthesis methods to a great extent. Spinel $Li_4Ti_5O_{12}$ can be synthesized by different synthesis techniques including solid-state reaction [6–8], sol–gel [9–11], high-energy ball milling [12], hydrothermal method [13,14], spray pyrolysis method [15], etc. Solid-state methods have some disadvantages, such as high calcination temperature, large particle size, impurity phases and lack of stoichiometry control. Compared to solid-state reaction, high-energy ball milling as a promising way can be used to synthesize micro- or nano-structured high-performance materials for a wide range of applications. It mainly utilized the mechanical energy

*Corresponding authors at: National Engineering Research Center for Nanotechnology, No. 28 East, Jiangchuan Road, Shanghai 200241, China. Tel.: +86 21 34291286; fax: +86 21 34291125.
E-mail addresses: zhangchm2003@163.com (C. Zhang), hdnbill@sh163.net (D. He).

0272-8842/$ - see front matter © 2013 Elsevier Ltd and Techna Group S.r.l. All rights reserved.
http://dx.doi.org/10.1016/j.ceramint.2013.09.038

originating from the constant collisions between particles and balls and bowl as mediums to meliorate the performance of materials or promote a solid state reaction. As compared to other ball-milling processes, high-energy ball milling was more efficient on enhancing the reaction rate or modifying the particle morphology of materials. Hence, the high-energy ball milling method is often used to obtain more homogenous powder. On the other hand, the reactant size also shows significant influence on the morphology and properties of the product [16,17]. In order to obtain the electrode materials with the best electrochemical performance, in this study, the $Li_4Ti_5O_{12}$ powders were synthesized by a high-energy ball milling assisted solid-state reaction and the TiO_2 particle size was also discussed to optimize the process parameters. The influence of TiO_2 particle size on the morphology and the electrochemical performance of $Li_4Ti_5O_{12}$ were systematically investigated.

2. Experimental

A series of $Li_4Ti_5O_{12}$ powders were synthesized by a high-energy ball milling assisted solid-state reaction. In this study, Li_2CO_3 (AR) and TiO_2 (anatase) powders with a particle size of 5–10 nm, 25 nm and 60 nm were applied as the raw materials for the Li and Ti sources. Stoichiometric amount of TiO_2 and Li_2CO_3 was dispersed in the mixture solution of alcohol and deionized water and then well mixed by high-energy ball milling using agate balls and bowl at a ball-to-powders weight ratio of 3:1. The milling was performed in air at 400 rpm rotational speed for 10 h. The white slurry was dried and further calcined under open air at 800 °C for 10 h to obtain the final white products. The obtained $Li_4Ti_5O_{12}$ powders prepared with a particle size of 5–10 nm, 25 nm and 60 nm TiO_2 powders were labeled as LTO-1, LTO-2 and LTO-3, respectively.

The crystal structure of the synthesized powders was examined by X-ray diffraction analysis (XRD, Model X'TRAX) using nickel filtered Cu-Ka radiation (λ=0.1 5406 nm) over the 2θ range from 10° to 80°. The particle morphology of the powders was observed using an S-4800 field emission scanning electron microscopy (SEM). The specific surface area of the samples was determined by N_2 adsorption using a 3H-2000 specific surface area instrument (Beishide Instrument-ST Co., Ltd., Beijing, China). The samples were treated at 200 °C for 3–5 h in a vacuum to remove the surface adsorbed species. Electrochemical properties of the samples were measured with the assembled coin cells, for which Li metal was used as a counter and reference electrode, the electrolyte was 1 M $LiPF_6$ in ethylene carbonate and diethyl carbonate (EC-DEC 1:1, v/v) and a Celgard2325 polypropylene micro-porous film was used as the separator. The $Li_4Ti_5O_{12}$ electrode was prepared by mixing 85 wt.% $Li_4Ti_5O_{12}$ active material, 10 wt.% carbon black (Super P) and 5 wt.% polyvynilidene fluoride (PVDF) binder dispersed in enough N-methyl-2-pyrrolidine (NMP). Then, the viscous slurry was cast on the current collector of a copper foil by a blade. After drying overnight under vacuum at 100 °C to remove the solvent, the electrode was punched to a disk shape with a diameter of 12 mm for the half-cell test. The cell was assembled in a dry glove box filled with high purity argon gas. The galvanostatic discharge–charge tests were carried out using a Neware Instrument in the voltage range of 1.0–3.0 V versus Li^+/Li. Electrochemical impedance spectroscopy was performed by an electrochemical workstation (Shanghai Chenhua Instrument Co. Ltd., China) in the frequency range from 1 MHz to 0.01 Hz.

3. Results and discussion

Fig. 1 displays the XRD patterns of the samples prepared with different particle sizes of TiO_2. All of the observed diffraction peaks conform to spinel $Li_4Ti_5O_{12}$ structure (JCPDS file no. 26-1198) without obvious impurity phase. The crystallite sizes of the samples are calculated based on the Scherrer formula $D = \beta \times \lambda / B \times \cos(\theta)$, where B is the full-width-at-half-maximum of the diffraction peaks, λ is the X-ray wavelength (0.15418 nm), β is a constant (0.89) and θ is the reflection angle of the peaks. Peaks at (111), (311) and (400) reflection are taken to evaluate the crystallite sizes of LTO-1, LTO-2 and LTO-3, respectively. The average crystallite sizes and the specific surface area of the samples are listed in Table 1. As shown in Table 1, the specific surface area of LTO-2 is larger than that of LTO-3. It is well known that there is a negative relationship between the particle size and the specific surface area. The result indicates that the reactant size plays an important role on $Li_4Ti_5O_{12}$. But the specific surface area of LTO-1 is smaller than that of LTO-2. The smaller specific surface area of LTO-1 may be attributed to the

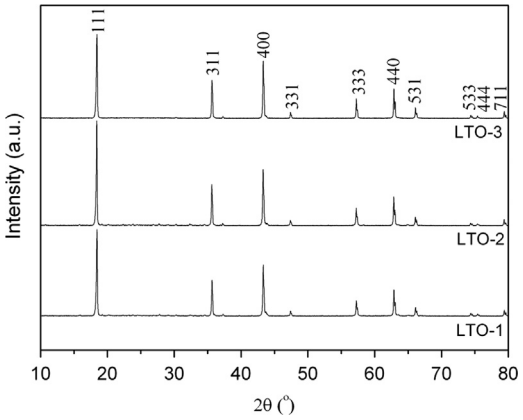

Fig. 1. XRD patterns of the $Li_4Ti_5O_{12}$ prepared with different particle sizes of TiO_2.

Table 1
Surface areas and crystallite sizes of the $Li_4Ti_5O_{12}$ powders.

Samples	Crystallite size (nm)	Surface area (m^2/g)
LTO-1	32.0	1.7087
LTO-2	39.5	2.5835
LTO-3	34.8	0.6323

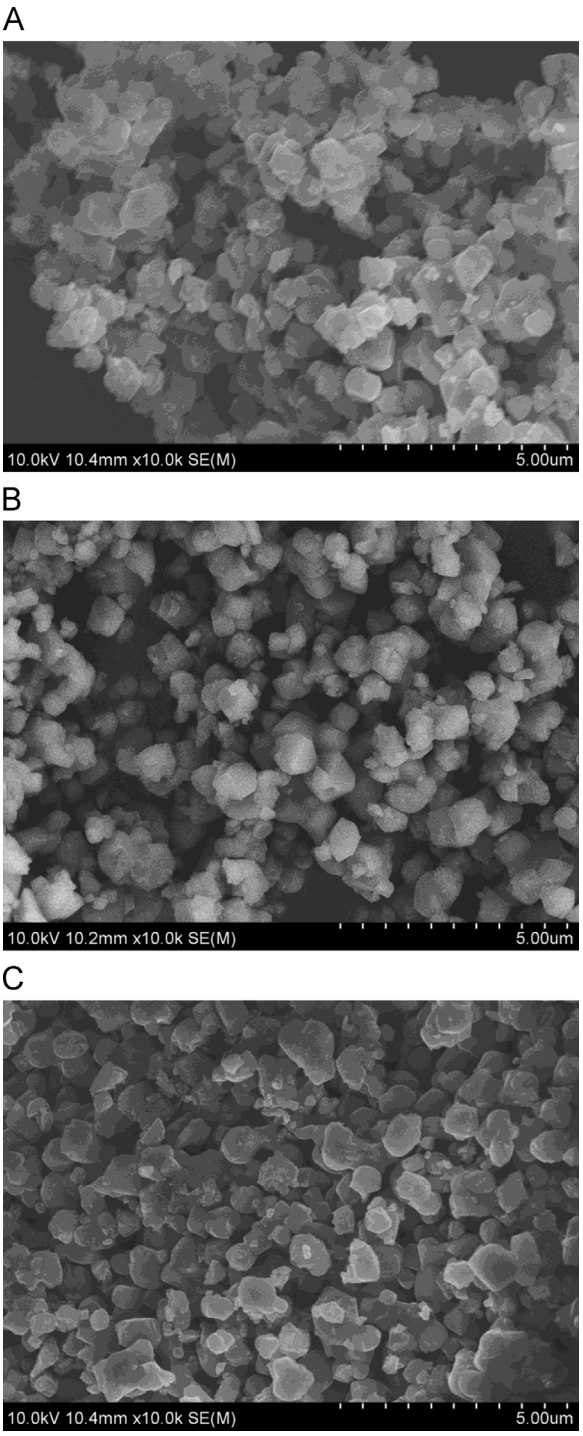

Fig. 2. SEM patterns of (a) LTO-1, (b) LTO-2 and (c) LTO-3.

aggregation of TiO_2. It also could be found that there is no distinct regularity between the particle sizes of TiO_2 and the crystallite sizes of the samples. The specific cause will be investigated subsequently.

In order to investigate the effect of the TiO_2 size on the morphology of $Li_4Ti_5O_{12}$, the field emission scanning electron micrographs of the synthesized LTO-1, LTO-2 and LTO-3 powders are shown in Fig. 2. From the figure, it can be seen that all the samples display uniform fine particles with the size within the range of 300–800 nm and the particle size of LTO-3 is the largest. In addition, the surface of the $Li_4Ti_5O_{12}$ particles is relatively smooth and evenly dispersed in most of the display area. It suggests that the high-energy ball milling method can decrease the particle size and prevent the aggregation of $Li_4Ti_5O_{12}$ particles. It is well known that the agglomerated particles can make the lithium ion insertion/extraction in individual $Li_4Ti_5O_{12}$ grains inhomogeneous. The $Li_4Ti_5O_{12}$ grains inside the densely packed particles might be inactive especially when cycled at high current densities due to the increased lithium ion diffusion distance. Furthermore, it is also found in Fig. 2 that compared with LTO-1, LTO-2 shows smaller particle size and better dispersion. The results indicate that the initial size of TiO_2 could affect the particle size and the surface areas of the final products.

The electrochemical properties of the powders are determined by the charge–discharge test at constant current density. The first discharge–charge curves of the $Li_4Ti_5O_{12}$ powders at different rates from 0.5 to 40 C in the potential window between 3.0 and 1.0 V are shown in Fig. 3. All samples exhibit extremely flat discharge–charge plateaus from 0.5 C to 2 C. The discharge–charge plateau potentials at 0.5–2 C are very close to the reversible redox potential of spinel $Li_4Ti_5O_{12}$ (1.55 V), as reported by Scharner et al. [18]. However, with the rate increasing, the discharge–charge plateau is obviously shortened and even no obvious discharge–charge plateaus can be found at 20 C and 40 C. The main reason is perhaps due to high resistance of the electrode, which causes the high polarization of the electrode. As shown in Fig. 3, compared with LTO-1 and LTO-3, the LTO-2 sample exhibits the best rate capability, especially at high rates. The LTO-2 presents a discharge capacity of 164.7 mAh/g at 0.5 C. In contrast, the discharge capacities of the LTO-1 and LTO-3 are lower as 159.7 and 155.8 mAh/g ,respectively. In addition, with the discharge–charge current rate increasing, the difference between the discharge capacities of samples becomes even more obvious. At 40 C, the capacities of the LTO-1 and LTO-3 are only 22.7 and 24.5 mAh/g, respectively; however, the discharge capacity of the LTO-2 still reaches 32.1 mAh/g. Hao et al. [19] reported that the particle size of electrode materials showed great influence on the electrochemical properties. As the nano-sized particle can reduce the ion-diffusion pathway, thus favoring lithium-ion mobility, the capacity can be improved significantly. Too large particle size of TiO_2 will lead to the longer Li ion extraction/insertion path and reduce the electronic diffusivity of $Li_4Ti_5O_{12}$. On the other hand, too small particle size of TiO_2 will cause the $Li_4Ti_5O_{12}$ particles agglomerated. It can be concluded that the excellent rate capability of LTO-2 could be attributed to the suitable particle size of TiO_2. Therefore, the result suggests that the particle size of TiO_2 plays an important role on the electrochemical properties of $Li_4Ti_5O_{12}$.

Long term cycling behaviors of the samples at different rates from 10 C to 40 C are also investigated and the results are shown in Fig. 4. Compared with LTO-1 and LTO-3, the sample LTO-2 exhibits the best cycling stability. The delithiation capacities of LTO-2 after 50 charge–discharge cycles are 70.6, 47.2 and 33.1 mAh/g at 10 C, 20 C and 40 C, respectively. The

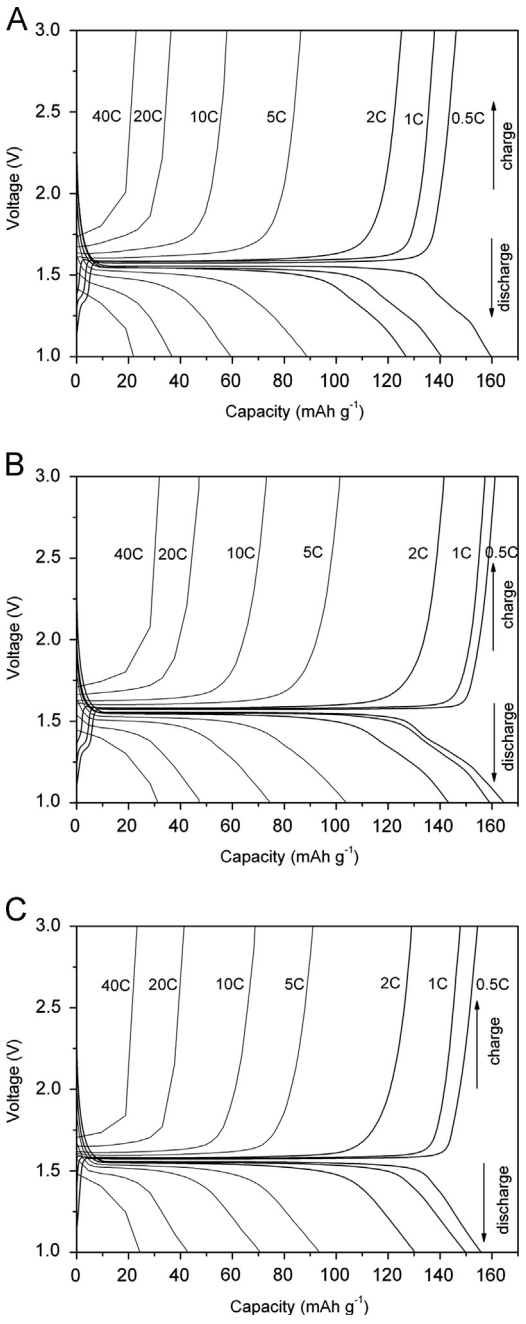

Fig. 3. The discharge–charge curves in the first cycle at different rates of the $Li_4Ti_5O_{12}$ electrodes prepared from (A) LTO-1, (B) LTO-2 and (C) LTO-3.

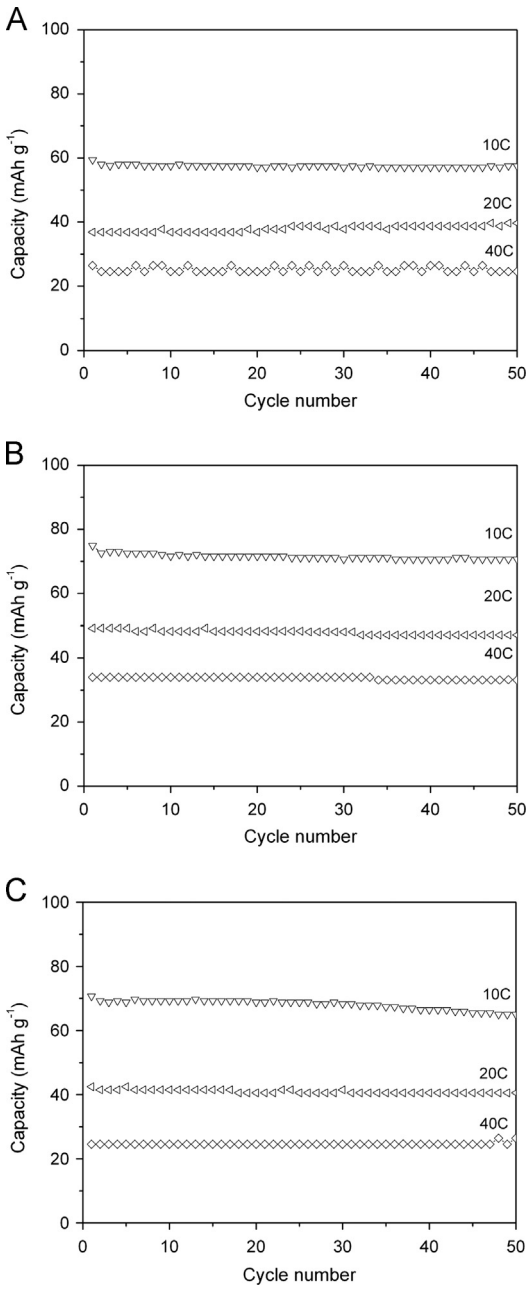

Fig. 4. The cyclic performance of the $Li_4Ti_5O_{12}$ electrodes prepared from (A) LTO-1, (B) LTO-2 and (C) LTO-3 at different rates.

corresponding capacity fading rates at these rates are calculated to be 0.11%, 0.08% and 0.05% per cycle, which shows very high capacity retention. The excellent performance and cycling stability is attributed to the high dispersion structure and the small particle size of this sample. From Fig. 4, it could be clearly seen that the capacity-cycle profile of LTO-1 shows a large fluctuation in capacity, which is not as smooth as that of the other two samples, especially at 40 C. As shown in Fig. 2(a), the LTO-1 sample owns more aggregated particles. We believe that a large portion of LTO-1 grains in the aggregated particles cannot be fully utilized and become inactive due to a longer diffusion distance for the lithium ion and insufficient lithium ion diffusion at high rates, which inevitably decreases the discharge capacity. The lithium ion insertion/extraction mainly takes place on the surface of the large particles and individual lithium ion insertion/extraction in the aggregated particles at different cycles leads to the capacity fluctuation.

To further demonstrate the effect of TiO_2 size on the electrode performance, the electrochemical impedance spectroscopy (EIS) of $Li_4Ti_5O_{12}$ were measured. The EIS curves of $Li_4Ti_5O_{12}$ electrodes in the frequency range of 1 MHz to 0.01 Hz at room temperature are showed in Fig. 5. The impedance plots are composed of a depressed semicircle in the high frequency range and a spike in the low frequency range. It is well known that the cross-section value of

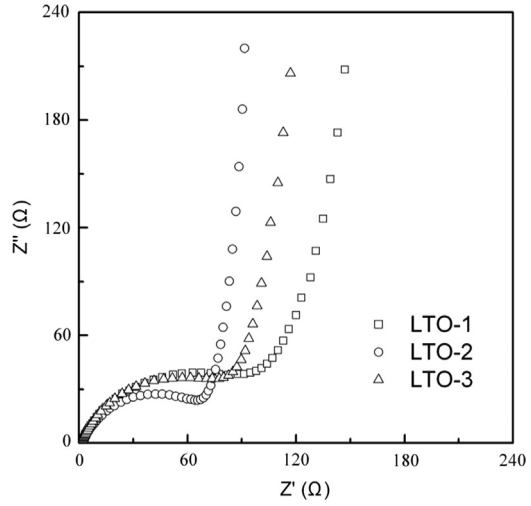

Fig. 5. Electrochemical impedance spectra results of $Li_4Ti_5O_{12}$ electrodes.

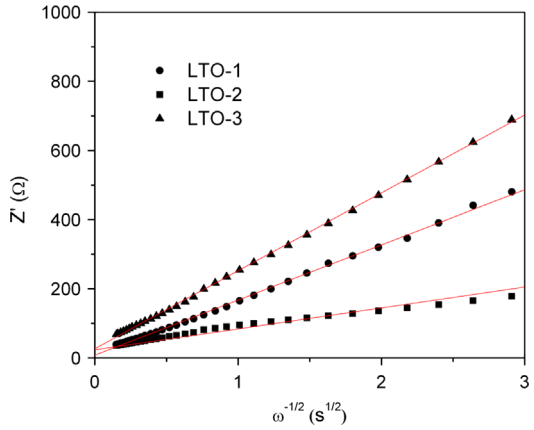

Fig. 6. Real impedance of $Li_4Ti_5O_{12}$ samples in low frequencies.

impedance spectra on the real Z'-axis at the high frequency is the internal resistance, while the semicircle is corresponding to the electrochemical reaction resistance and the double layer capacity of the electrode. The inclined line in the lower frequency range is attributed to the Warburg impedance, which is associated with solid-state diffusion of Li^+ through the $Li_4Ti_5O_{12}$ electrode [20]. As shown in Fig. 5, the LTO-2 electrode exhibits the lowest electrochemical reaction resistance, which is consistent with the result of the best reversible capacities.

From Fig. 6, we can obtain the value of the Warburg impedance coefficient (σ_w). According to the following two equations:

$$Z_{re} = R_s + R_{ct} + \sigma_w \cdot \omega^{-0.5} \quad (1)$$

$$D = 0.5\left(\frac{RT}{AF^2\sigma_W C}\right)^2 \quad (2)$$

where R_s is attributed to the ohmic resistance of the electrolyte; R_{ct} indicates the charge transfer resistance at the active material interface; ω is angular frequency in the low frequency region; D is the Li-ion diffusion coefficient; R is the gas constant; T is the absolute temperature; F is the Faraday's constant; A is the area of the electrode surface; C is the molar concentration of Li-ions, the D can be calculated.

Table 2
EIS simulation parameters of the $Li_4Ti_5O_{12}$ prepared with different particle sizes of TiO_2.

Samples	σ_w (Ω cm^2/s$^{0.5}$)	D (cm^2/s)
LTO-1	161.6	1.37E−14
LTO-2	159.5	1.41E−14
LTO-3	180.6	1.10E−14

As shown in Table 2, sample LTO-2 shows the highest ion conductivity. This should be ascribed to the fact that sample LTO-2 owns the largest surface area and the fewest particle agglomerations. It is well known that well-dispersed $Li_4Ti_5O_{12}$ can shorten the lithium-ion diffusion pathway, favoring lithium-ion mobility and enhancing high rate performance. From all of the above results, it is concluded that the LTO-2 presents the best electrochemical performance in our study which agrees well with that of the discharge–charge measurements. Therefore, particles size of TiO_2 should be optimized to supply the well dispersion for improving the electrochemical performance of the $Li_4Ti_5O_{12}$.

4. Conclusions

The $Li_4Ti_5O_{12}$ powders have been easily synthesized by a simple high-energy ball milling assisted solid-state method. The influences of the TiO_2 particle size are investigated in detail. The results show that the TiO_2 particle size could affect the grain size, the surface area, the electrochemical properties, the cyclic performance and the Li-ion diffusion coefficient of $Li_4Ti_5O_{12}$. All these demonstrate that the TiO_2 particle size plays an important role on the electrochemical properties of $Li_4Ti_5O_{12}$. The $Li_4Ti_5O_{12}$ synthesized by TiO_2 with particle size of 25 nm exhibits the best electrochemical properties. The discharge capacity reaches 164.7 mAh/g at 0.5 C. When the current rate increases to 10 C, the first discharge capacity is 70.6 mAh/g, and the capacity retention is 94.5% at the 50th cycle.

Acknowledgments

This work was supported by the National Science Foundation of China (no. 21171116) and International Science & Technology Cooperation Program of China (no. 2012DFG11660). The first author would also like to thank Dr. Ye Lin at University of South Carolina for offering help with discussion and revision.

References

[1] K.M. Colbow, J.R. Dahn, R.R. Haering, Structure and electrochemistry of the spinel oxides $LiTi_2O_4$ and $LiTiO_4$, Journal of Power Sources 26 (1989) 397–402.

[2] Y.P. Wu, Elke Rahm, Rudolf Holze, Effects of heteroatoms on electrochemical performance of electrode materials for lithium ion batteries, Electrochimica Acta 47 (2002) 3491–3507.
[3] G.F. Yan, H.S. Fang, H.J. Zhao, G.S Li, Y. Yang, L.P. Li, Ball milling-assisted sol–gel route to $Li_4Ti_5O_{12}$ and its electrochemical properties, Journal of Alloys and Compounds 470 (2009) 544–547.
[4] L.X. Yang, L.J. Gao, $Li_4Ti_5O_{12}$/C composite electrode material synthesized involving conductive carbon precursor for Li-ion battery, Journal of Alloys and Compounds 485 (2009) 93–97.
[5] X.B. Hu, Z.J. Lin, K.R. Yang, Z.H. Deng, J.S. Suo, Influence factors on electrochemical properties of $Li_4Ti_5O_{12}$/C anode material pyrolyzed from lithium polyacrylate, Journal of Alloys and Compounds 506 (2010) 160–166.
[6] S.W. Han, J.W. Shin, D.H. Yoon, Synthesis of pure nano-sized $Li_4Ti_5O_{12}$ powder via solid-state reaction using very fine grinding media, Ceramics International 38 (2012) 6963–6968.
[7] D. Wang, C.M. Zhang, Y.Y. Zhang, J. Wang, D.N. He, Synthesis and electrochemical properties of La-doped $Li_4Ti_5O_{12}$ as anode material for Li-ion battery, Ceramics International 39 (2013) 5145–5149.
[8] G.J. Wang, J Gao, L.J. Fu, N.H. Zhao, Y.P. Wu, T. Takamura, Preparation and characteristic of carbon-coated $Li_4Ti_5O_{12}$ anode material, Journal of Power Sources 174 (2007) 1109–1112.
[9] J. Wang, X.M. Liu, H. Yang, X.D. Shen, Characterization and electrochemical properties of carbon-coated $Li_4Ti_5O_{12}$ prepared by a citric acid sol–gel method, Journal of Alloys and Compounds 509 (2011) 712–718.
[10] C.M. Zhang, Y.Y. Zhang, J. Wang, D. Wang, D.N. He, $Li_4Ti_5O_{12}$ prepared by a modified citric acid sol–gel method for lithium-ion battery, Journal of Power Sources 236 (2013) 118–125.
[11] M. Venkateswarlu, C.H. Chen, J.S. Do, C.W. Lin, T.C. Chou, B.J. Hwang, Electrochemical properties of nano-sized $Li_4Ti_5O_{12}$ powders synthesized by a sol–gel process and characterized by X-ray absorption spectroscopy, Journal of Power Sources 146 (2005) 204–208.
[12] G.X. Wang, J.J. Xu, M. Wen, R. Cai, R. Ran, Z.P. Shao, Influence of high-energy ball milling of precursor on the morphology and electrochemical performance of $Li_4Ti_5O_{12}$–ball-milling time, Solid State Ionics 179 (2008) 946.
[13] H. Yan, Z. Zhu, D. Zhang, W. Li, Q. Lu, A new hydrothermal synthesis of spherical $Li_4Ti_5O_{12}$ anode material for lithium-ion secondary batteries, Journal of Power Sources 219 (2012) 45–51.
[14] Z.W. Zhang, L.Y. Cao, J.F. Huang, D.Q. Wang, J.P. Wu, Y.J. Cai, Hydrothermal synthesis of $Li_4Ti_5O_{12}$ microsphere with high capacity as anode material for lithium ion batteries, Ceramics International 39 (2013) 2695–2698.
[15] G.N. Zhu, H.J. Liu, J.H. Zhuang, C.X. Wang, Y.G. Wang, Y.Y. Xia, Carbon-coated nano-sized $Li_4Ti_5O_{12}$ nanoporous micro-sphere as anode material for high-rate lithium-ion batteries, Energy & Environmental Science 4 (2011) 4016–4022.
[16] H.P. Li, J.A. Stkhar, The influence of the reactant size on the micropyretic synthesis of NiAl intermetallic compounds, Journal of Materials Research 10 (1995) 2471–2480.
[17] D.T. Gillespie, S. Lampoudi, L.R. Petzold, Effect of reactant size on discrete stochastic chemical kinetics, Journal of Chemical Physics (2007) http://dx.doi.org/10.1063/1.2424461.
[18] S. Scharner, W. Weppner, P. Schmid-Beurmann, Evidence of two-phase formation upon lithium insertion into the $Li_{1.33}Ti_{1.67}O_4$ spinel, Journal of the Electrochemical Society 146 (1999) 857–861.
[19] Y.J. Hao, Q.Y. Lai, J.Z. Lu, H.L. Wang, Y.D. Chen, X.Y. Ji, Synthesis and characterization of spinel $Li_4Ti_5O_{12}$ anode material by oxalic acid-assisted sol–gel method, Journal of Power Sources 158 (2006) 1358–1364.
[20] J.J. Huang, Z.Y. Jiang, The preparation and characterization of $Li_4Ti_5O_{12}$/carbon nano-tubes for lithium ion battery, Electrochimica Acta 53 (2008) 7756–7759.